Ti-Peroxo Species in the TS-1/H_2O_2/H_2O System

Francesca Bonino, Alessandro Damin, and Gabriele Ricchiardi

Department of Inorganic, Physical and Material Chemistry, University of Turin, Via P. Giuria 7, 10125 Torino, Italy, and INSTM sezione di Torino Università, 10125 Torino, Italy

Marco Ricci, Guido Spanò, and Rino D'Aloisio

Polimeri Europa S.p.A., Istituto G. Donegani, Via G. Fauser 4 I-28100, Novara, Italy

Adriano Zecchina, Carlo Lamberti,* Carmelo Prestipino, and Silvia Bordiga

Department of Inorganic, Physical and Material Chemistry, University of Turin, Via P. Giuria 7, 10125 Torino Italy, INSTM sezione di Torino Università, 10125 Torino, Italy, and INFM UdR di Torino Università, 10125 Torino, Italy

Received: July 24, 2003; In Final Form: October 30, 2003

This work is devoted to the study of the active species present on the TS-1-H_2O_2/H_2O catalytic system and to the elucidation of the mechanisms of formation and interconversion of these species. In particular new experimental data and computational evidence are reported concerning (i) the acidic character of hydroperoxo species, (ii) the role of water in the hydroperoxo−peroxo interconversion, and (iii) the role of water as co-reactant in favoring the H_2O_2 adsorption at Ti sites. It is demonstrated that gentle drying of the TS-1-H_2O_2/H_2O system leads to the transformation of the yellow peroxo groups into noncolored species, still located at Ti centers. The process is reversible and the colored species can be partially restored again by successive rehydration. As the hydroperoxo and peroxo species have different oxidizing ability, these results indicate that the presence of water molecules at hydrophilic Ti sites can correlate with the catalytic activity. As it is well-known, hydroperoxo and peroxo species are unstable and their concentration declines with aging. However, UV−vis spectroscopic results demonstrate that small fractions of peroxo species (characterized by a cream color) persist on the sample even after prolonged aging. On this basis and on EXAFS results, a comprehensive scheme of the formation and mutual conversion of oxidized species is concluded. Spectroscopic results, supported by acidity measurements and titration of active oxygen content, show the following: (i) the O−O species, responsible to the yellow color of the catalyst, is a side-on peroxo complex, probably generated by the reversible rupture of one Ti−O−Si bridge, with the formation of Ti(O_2H) and H−O−Si groups; (ii) the stability of this peroxo complex is low in the absence of an excess of H_2O; (iii) a strong enhancement of the acidity of the TS-1/H_2O_2/H_2O system with respect to that of TS-1/H_2O has been observed, demonstrating a synergic role between Ti(IV) centers and hydrogen peroxide; and (iv) a small fraction of oxidized species has a negligible oxidizing ability and probably does not play any role in the catalysis.

1. Introduction

Titanium silicalite-1 (TS-1) is a synthetic zeolite[1] in which a small number of Ti atoms substitute tetrahedral Si atoms in a purely siliceous framework with the MFI structure.[2] It is an active and highly selective catalyst in a number of low-temperature oxidation reactions, with aqueous H_2O_2 as the oxidant agent. We will mention the following: the conversions of ammonia to hydroxylamine, of secondary alcohols to ketones, and of secondary amines to dialkylhydroxylamines or reactions such as phenol hydroxylation, olefin epoxidation, or cyclohexanone ammoximation.[3,4] This explains why it has been one of the most studied materials in heterogeneous catalysis in the last two decades on both experimental[5−31] and computational[6,12,27,29−30,31−41] grounds. Among the experimental papers we can distinguish vibrational spectroscopies (both IR and Raman),[6−13,16,27−30] UV−vis spectroscopy,[7,12,14a,17,18,26,29] X-ray absorption spectroscopies (both EXAFS and XANES),[12,14−17,19,20,22,23,29] EPR[26,27] spectroscopy, and microcalorimetric[23,29] and powder diffraction (using both X-rays and neutrons)[5] studies. Quoted theoretical studies have focused on different aspects of the reactivity of the catalyst: vibrational properties,[12,28−30,32−34] hydrolysis of Ti−O−Si bridges,[36] interaction with guest molecules,[28−30,32,33,35] and stability of different O−O moieties on Ti(IV) species.[6,31,37−39,41]

SCHEME 1

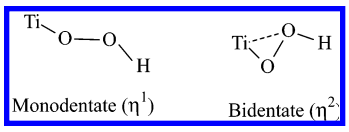

Despite the numerous papers describing the catalytic activity of TS-1, only a few works have tried to investigate the nature and the properties of the active species formed in TS-1 upon interaction with H_2O_2. This lack can be ascribed to severe experimental problems, mainly due to the presence of H_2O

* Address correspondence to this author. Fax: +39011-6707855. E-mail: carlo.lamberti@unito.it.

10.1021/jp036166e CCC: $27.50
Published on Web 02/18/2004

SCHEME 2

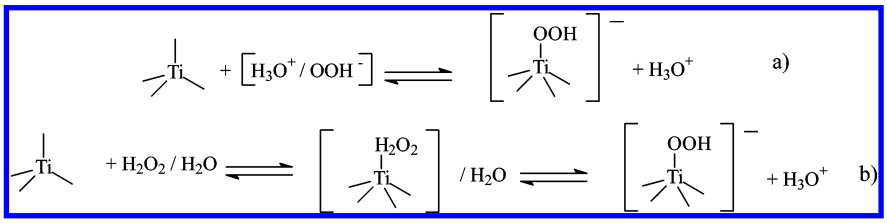

SCHEME 3

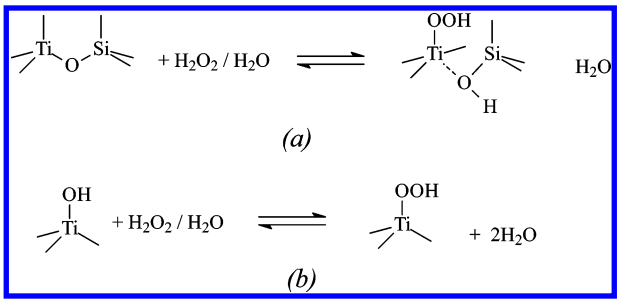

(which precludes the extended use of IR spectroscopy) and of the lability of complexes formed by H_2O_2 on Ti(IV) centers in TS-1. The most used technique is UV−vis DRS spectroscopy because it is not affected by the presence of H_2O. This technique has revealed the formation, upon contact with H_2O_2 water solution, of a new LMCT band from the O−O moiety to the Ti center, appearing around 26 000 cm^{-1} (385 nm).[13,16,21,22,26] Other papers appeared with use of EPR,[26,27] IR,[6,8] Raman,[6,13] EXAFS,[22,31] and computational[6,31,37−39,41] approaches to investigate the complexes formed upon dosing H_2O_2 (or more complex species such as *tert*-butyl hydroperoxide) on titanosilicates. This is the reason, after more than 20 years from the discover of the material, the detailed structure of the O−O species formed at the catalytic center, which is thought to be the active intermediate in partial oxidation reactions, is still debated. The species which can be generated at Ti sites upon H_2O_2/H_2O contact can have neutral (coordinated H_2O_2), peroxidic, superoxidic, and hydroperoxidic character. The most popular view is that the active species is a Ti-hydroperoxide that may be either monodentate (η^1) or bidentate (η^2)[3b,6,8,16,41] (see Scheme 1) even if the other hypothesized structures cannot be ruled out. Hydroperoxidic η^1 or η^2 complexes can be formed by interaction of Ti(IV) with a HO_2^- anion (the pK_a of the $H_2O_2 + H_2O \rightleftarrows HO_2^- + H_3O^+$ equilibrium being 11.8 in water at 20 °C, a value comparable to the third dissociation constant of H_3PO_4) following Scheme 2a. Deprotonation of the H_2O_2 molecule on the Ti(IV) site itself (Scheme 2b) is another mechanism leading to Ti-hydroperoxidic species. The latter mechanism can also occur either on a perfect [Ti−(O−Si)$_4$] site by rupture of one of the four Ti−O−Si bridges or on a defective [(H−O)−Ti−(O−Si)$_3$] site by elimination of a water molecule (see Scheme 3 a,b). Unfortunately, there is no Ti-hydroperoxo compound of known structure to be used as a model. Conversely, the structures of several Ti-peroxo complexes are known from diffraction studies,[42] all of them showing the side-on η^2 geometry. None of these compounds is known to be active in partial oxidation reactions.[43] Similar consideration can be addressed for the Ti(IV)-substituted Keggin polyoxotungstate compound.[44]

Concerning peroxo complexes, it is worth noticing that they can be formed in TS-1 by evolution of both η^1 and η^2 hydroperoxo complexes upon further deprotonation in the presence of water with formation of H_3O^+/H_2O. Very recently some of us have proven, exploiting a resonant Raman effect,

SCHEME 4

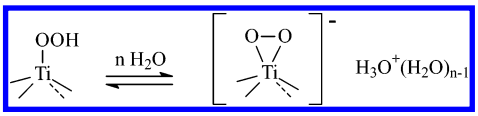

that the Ti(OO) species peculiar of the yellow color of the TS-1/H_2O/H_2O_2 system is a Ti-peroxo species in η^2 configuration.[13] On this basis the following question arises: Is the Ti-peroxo species formed in TS-1 a peculiarly active one or do we have to hypothesize its constant equilibrium and hence conversion into a hydroperoxo active species for instance following Scheme 4? Considering this debate, the identification of the Ti(OO) species present in the TS-1/H_2O/H_2O_2 system and the understanding of how their equilibrium and stability are influenced by water molecules becomes the key point.

2. Experimental Section

2.1. Synthesis. A TS-1 sample has been synthesized in EniChem (now Polimeri Europa) laboratories following a procedure described in the original patent.[1] The Ti content, expressed in TiO_2 wt %, has been found to be 2.76. For comparison also a Ti-free silicalite has been synthesized under the same conditions. The complete insertion of Ti atoms in the MFI framework has been proved by comparison of the amount of Ti determined by chemical analysis with the cell volumes obtained by Rietveld refinement of powder XRD data.[5] The absence of extraframework TiO_2 particles has been confirmed by UV−vis and XANES spectroscopies and by the absence of the 144 cm^{-1} Raman band. The TS-1 sample has been measured in contact with a 30% H_2O_2 aqueous solution, representing the working conditions of the catalyst.[3,4] For blanc experiments an amorphous silica (Aerosil 300) and a Ti-free Silicalite-1 (a purely siliceous zeolite with the same MFI lattice than TS-1) have been used.

2.2. Characterization Techniques. The diffuse reflectance UV−vis spectra were obtained on a Perkin-Elmer spectrophotometer. Spectra colleted with this instrument, DRS(λ), will not be reported using the Kubelka−Munk function, conventional in diffuse reflectance spectroscopy, but just as the ratio between the spectrum of the sample, $S(\lambda)$, and that of the blank reference, $B(\lambda)$, $BaSO_4$ in our case:

$$\mathrm{DRS}(\lambda) = 100S(\lambda)/B(\lambda) \qquad (1)$$

This choice has been dictated by the fact that (i) one of the main goals of this work is the study of the effect of the amount of water on the nature, evolution, and stability of the peroxo complex(es) formed on TS-1 and (ii) the amount of water, filling the empty spaces between adjacent crystallites of the zeolite powder, strongly affects the scattering properties of the sample. The filling of intercrystalline voids by liquid water causes a decrease of the difference of refraction index between crystallites and intercrystalline spaces, penalizing the scattering processes and resulting in a deeper penetration of the beam inside the sample. A decrease of the scattering by crystallites causes a

reduction of the fraction of reflected photons that is actually able to reach the detector, and leads to an apparent increase of the sample absorption. This unavoidable experimental artifact has a nonlinear magnification when Kubelka−Munk units are adopted; conversely, its effect can be correctly evaluated if spectra are reported according to eq 1. For all UV−vis DRS spectra, besides the charge-transfer region (210−550 nm), also the region of the overtones and combination modes of H_2O (1250−2000 nm) will be reported, to allow a direct evaluation of the amount of water present on the sample.

EXAFS/XANES spectra have been performed in the transmission mode, at the EXAFS13 beam line of the DCI storage ring (operating at 1.85 GeV with a typical current of 300 mA) of LURE laboratories in Orsay (France), using air-filled ionization chambers for both incident and transmitted beams. For both detectors the gas pressure has been optimized ad hoc for each sample, maximizing the measured current within the linearity region of the device. The incident beam was monocromatized by using a double crystal Si(111) (Si(311)) with a sampling step of 2.0 (0.5) eV and an integration time of 2.0 (1.0) s/point for EXAFS (XANES). The energy/angle calibration was performed with a Ti foil and crystals were detuned up to $^1/_2$ of the rocking curve to avoid harmonics. The homogeneity of the pellets was controlled by the uniformity of the X-ray beam transmitted through the sample by radiographic methods. Measurements have been performed with a liquid nitrogen cryostat since exposure of the sample to the synchrotron radiation beam decomposes the Ti-peroxo at room temperature. This operation is, however, not trivial because the procedure of cryostat evacuation with a rotary pump, usually performed before starting the cooling procedure, resulted in the desorbtion of the OO complex on Ti(IV) species, as testified by the pellet color, which changed from yellow to white. We have therefore cooled the sample temperature below 0 °C first, evaluated the cryostat second, and terminated the cooling procedure down to the liquid nitrogen temperature. For TS-1 sample in each condition (in a vacuum or in the presence of H_2O or of H_2O/H_2O_2 solutions) the EXAFS spectrum was acquired four times under the same experimental conditions: from the four extracted $\chi_i(k)$ ($i = 1, 2, 3, 4$) the average $\chi(k) = {}^1/_4\sum_{i=1}^4 \chi_i(k)$ function was computed and used for the data analysis. The $\chi_i(k)$ extraction form raw μx spectra has been performed according to the procedure described in section 2.1 of ref 45. The analysis of the EXAFS data has been carried out with programs developed by Michalowicz[46] and following standard procedures[47] in the frame of single scattering theory fitting only the first shell environment around Ti. For the sample measured in vacuo the first shell is constituted by framework oxygen atoms only, while also the OO moiety is present upon contact with H_2O/H_2O_2 solutions. Ti−O phase and amplitude functions have been extracted from the TiO_2 (anatase) model compound, as was already done in previous EXAFS experiments on TS-1 catalyst.[14,16,17,19,22,23]

The active oxygen content has been measured as follows. TS-1 or silicalite-1 samples (ca. 2 g) and hydrogen peroxide (typically 15−20 mL of 1−5% aqueous solutions) were magnetically stirred at room temperature for a few minutes. Then the solid was filtered and quickly dried on a porous plate, thus obtaining a yellow (TS-1) or white (silicalite-1), free-flowing powder. Approximately 0.2 g of this powder was suspended in 20−30 mL of acidic (H_2SO_4) water containing an excess of potassium iodide, and a few drops of a 3% aqueous solution of ammonium molybdate were added. Within seconds, oxidation of iodide occurred and the produced iodine was titerd with a 0.1 N solution of sodium thiosulfate, using a starch solution as an indicator.

Titration of acidity has been accomplished by means of conventional base addition with Metrohm 718 STAT *titrino* equipment. TS-1 (0.2 g, 2.76 wt % of TiO_2) was suspended in H_2O and added to 2.1 mL of 0.032 M H_2O_2 solution (prepared from a commercial stabilized 36 vol solution). The starting volume of the suspension was 12.1 mL. pH was monitored with a standard glass electrode under stirring until equilibration. NaCl (0.04 g) was added, resulting in a lowering of the pH due to ion exchange with acid sites inside the zeolite pores. This pH value is given as the starting point of the titration curves presented below. NaOH (Carlo Erba NORMEX 0.05 N) has been progressively added while monitoring the pH until it reaches 8. Although the true final point of the titration may occur at higher pH values, these were not investigated due to the instability of the pH caused by hydrolysis reactions.[53,54] Blank experiments were conducted under the same conditions, on silicalite-1 and amorphous silica (Aerosil 300), with and without hydrogen peroxide addition. The acidity of the H_2O_2 solution itself was also titrated as a reference.

2.3. Models and Computational Details. We have used a cluster model obtained by cutting the MFI framework around the T1 site and including 16 tetrahedral units to simulate the Ti site in TS-1 and to study its interaction with H_2O_2. This cluster is the same used in ref 28 in the study the interaction with pyridine and acetonitrile and is among those used in refs 29, 30, and 32 in the study the interaction with water and ammonia. Following the already published literature it will be called MFI_T16.

To limit the computational demand in our calculations, the cluster/embedded cluster ONIOM[48] scheme, based on the integration of molecular orbital at different levels of theory,[48b] was adopted with the same scheme employed in refs 28−30 and 32. The total energy of the ONIOM system, E(ONIOM), is obtained from three distinct self-consistent-field energy calculations which are combined according to E(ONIOM) = E_{High}(model zone) + [E_{Low}(whole cluster) − E_{Low}(model zone)], with (i) E_{Low}(whole cluster) being the energy of the whole cluster calculated at the low level of theory (RHF/3-21G(H,N,C,Si,O), 3-21G*(Ti)), (ii) E_{Low}(model zone) the energy of the model zone computed at the low level of theory (RHF/3-21G(H,C,N,Si,O), 3-21G*(Ti)), and (iii) E_{High}(model zone) the energy of the model zone computed at the high level of theory at (B3-LYP/6-311+G-(d,p)(H,C,N,Si,O), *ppp*(Ti)) high (H) level. Note that *ppp* represents the basis set employed for the Ti atom, which is composed of effective small core pseudopotentials[49] + LANL2DZ[49] + Ahlrichs TZV "p" polarization function.[50] In cluster MFI_T16 the model zone (stick and balls in Figure 5a) corresponds to the T5 model (brutto formula $Ti(SiOH_3)_4$) employed in refs 29, 32, and 39. During the optimization cycles all atomic positions were free to relax without any artificial constraints imposed on the model zone except for those induced by the whole cluster itself. This role is played by the link atoms which transfer mechanical constraints from the whole cluster to the model zone. In fact, link atoms are forced to stay along the Si−O directions (where Si is the last atom of the model zone and O is the first atom of the zone treated at the lower level).

According to the nomenclature adopted in refs 28−30 and 32, the four first shell O atoms are divided into one apical (O_{ap}) and three equatorial (O_{eq}) depending on whether they are in the opposite direction of the adsorbed molecule or not. Adsorption of H_2O_2 splits the 6 O−Ti−O angles of the TiO_4 unit

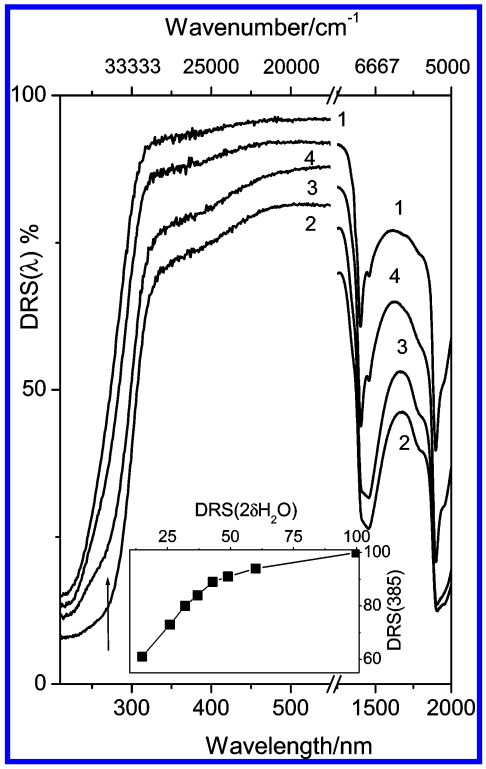

Figure 1. DRS spectra of TS-1 in different conditions (plotted as percentage) of the ratio between the reflectance of the sample and that of a $BaSO_4$ blank: $DRS(\lambda) = S(\lambda)/B(\lambda)$. Left and right parts refer to the UV−vis and NIR regions, where LMCT transitions and water modes are present, respectively. Sample as such, measured without activation, curve 1; after having been contacted with water drops, curve 2. Curves 3 and 4 report the effect of water desorption upon time elapse in air (24 h and 7 days, respectively). The inset reports the value of the DRS function measured at 385 nm as a function of the value at 1400 nm (proportional to H_2O content). This experimental relationship will be used to evaluate a background correction of the DRS spectra at $\lambda =$ 385 nm for the TS-1/H_2O_2/H_2O system (vide infra Figures 2 and 3 and Table 2).

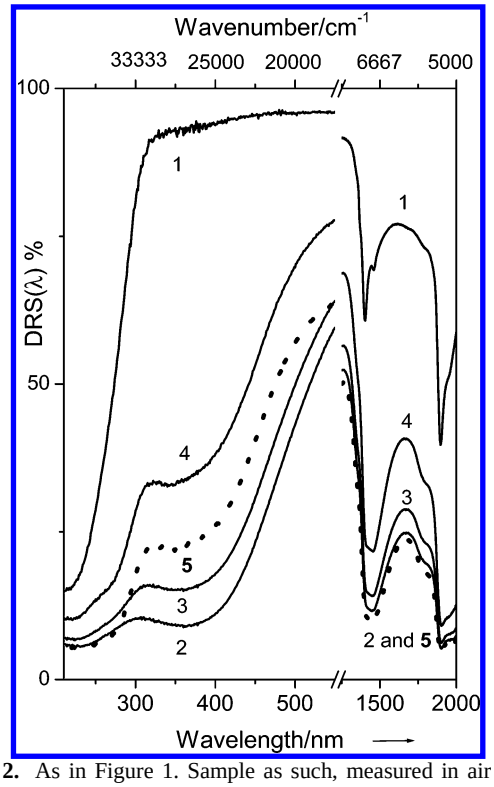

Figure 2. As in Figure 1. Sample as such, measured in air without activation, curve 1; after contact with H_2O_2/H_2O (30%) solution, curve 2. Curves 3 and 4 report the effect of time elapse (10 and 24 h, respectively). Curve 5 refers to the spectrum collected after spectrum 4 upon contact with H_2O.

(109.5° in perfect T_d symmetry) into two triplet $O_{eq}-Ti-O_{eq}$ and $O_{eq}-Ti-O_{ap}$ angles which will be labeled α and β, respectively. CM defines the center of mass of the three O_{eq} atoms.[51] The a posteriori method proposed by Lendvay and Mayer[52] has been used to estimate the basis set superposition error (BSSE). From the ONIOM computed binding energies (BE), the BSSE corrected binding energies (BE^c) are obtained as $BE^c = BE - BSSE$.

3. Results

3.1. UV−Vis Spectroscopy. Figure 1 reports the time evolution (curves 3 and 4) of the UV−vis DRS spectra of TS-1 after interaction with water from the liquid phase (curve 2). Curve 1 reports, for comparison, the spectrum before contact with ligand water. The zeolite was not previously activated and thus still contains a fraction of water molecules adsorbed from the ambient in spectrum 1. In such conditions the spectrum is characterized by a $Ti^{4+}O^{2-} \rightarrow Ti^{3+}O^-$ ligand-to-metal charge transfer (LMCT) slightly red shifted with respect to that measured on the activated material: 220 vs 208 nm (45 000 vs 48 000 cm^{-1}).[7,12,14a,17,18,26,29] In the NIR region two complex features are clearly observed around 1400 nm (7140 cm^{-1}) and 1900 nm (5260 cm^{-1}) due to the overtone of the ν and to the combination of ν and δ modes of physisorbed water, respectively. The soaked sample (spectrum 2) is characterized by a further red shift of the $Ti^{4+}O^{2-} \rightarrow Ti^{3+}O^-$ LMCT, now around 285 nm (35 000 cm^{-1}), by the evident increase of the water modes in the NIR region and by a consistent reduction of the DRS(λ) signal in the whole 300−550-nm range. As an example, around 385 nm (26 000 cm^{-1}), the DRS(λ) function moves from DRS(385) = 94 to 73%. This important reduction is not ascribable to an increased absorption of the radiation in the 300−550-nm range (no new LMCT component is expected in that region for the TS-1/H_2O system) but to a decrease of the scattering power of the sample caused by the presence of a liquid phase in the space between adjacent zeolite crystals (see the Experimental Section). The progressive evaporation of such water molecules (spectra 3 and 4) causes the progressive convergence to the initial conditions (spectrum 1). The LMCT region of spectrum 3 becomes resolved and a shoulder at 270 nm (37 000 cm^{-1}) is now evident (see arrow). The structured nature of the spectrum reflects the heterogeneity of oxygen atoms in the first coordination sphere around Ti(IV): chemically bonded framework atoms and weakly interacting atoms of the physically adsorbed water molecules.[29] According to Ricchiardi et al.,[36b] who have suggested a different affinity of the 12 different T sites toward water molecules, resulting in 5- and 6-fold coordinated complexes, also the simultaneous presence of Ti(IV) sites coordinating one or two water molecules could explain the presence of structured features in spectrum 3. The change in the scattering background does not allow us to appreciate such a fine structure in spectrum 2.

Spectra 1−4 of Figure 2 report the same experiment obtained by dosing an H_2O_2/H_2O solution (30 wt %) on TS-1. Upon contact with H_2O_2 water solution (spectrum 2), a new LMCT band appears around 385 nm (26 000 cm^{-1}).[13,16,22,26] This band has already been assigned to the η^2 peroxo moiety to the Ti center[13] even if some authors believe that O^{2-} species are also contributing to this absorption.[27] The position of this component (visible region) reflects the strong interaction between the Ti-

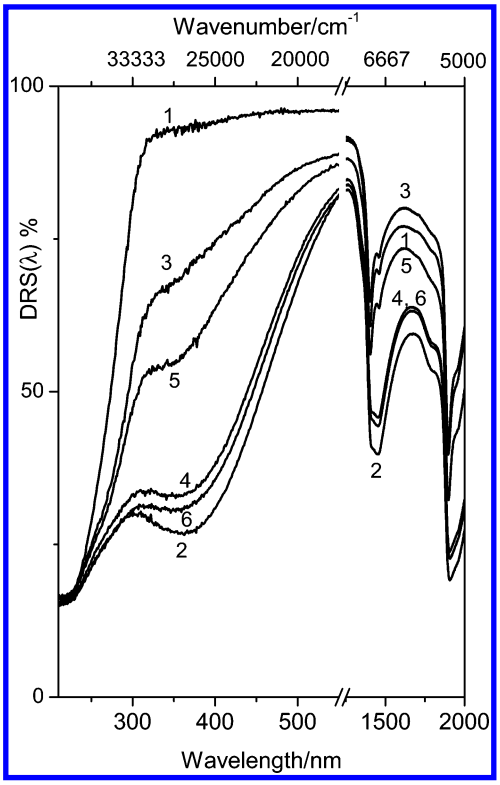

Figure 3. As in Figure 1: aging/restoration cycles. Sample as such, measured without activation, curve 1; after contact with H_2O_2/H_2O (30%) solution, curve 2. Curve 3 reports the effect of long time elapse (15 days). A second and a third contact H_2O_2/H_2O (30%) solution drop is reported in curves 4 and 6, respectively, together with the intermediate aging of 1 day after the second contact (curve 5).

(IV) center and the peroxo ligand. The corresponding DRS-(385) value becomes only 10% (see Table 2), suggesting that this species is abundant. In the NIR region, the evolution in time (spectra 3 and 4) reflects the progressive water desorption, which is accompanied by the parallel decrease of the 385-nm component (whose DRS(385) function increases to 16% and 35%, respectively). It is clear that the Ti colored peroxo complexes are progressively consumed; however, the decrement as a function of time cannot be directly quantified, as a consequence of the large variation of the sample scattering with water desorption (see Figure 1 and related discussion). We will return to this important point in the Discussion. In spectrum 4, the change in the scattering background allows us to appreciate a feature again around 270 nm (37 000 cm^{-1}), compared with spectrum 3 of Figure 1. Finally, spectrum 5 reports the effect of dosing a drop of water on the sample immediately after detection of spectrum 4. The addition of water magnified the intensity of the 385-nm band, moving the DRS(385) from 35% to 24% (see Table 2). This fact must be considered with care, because a fraction of this effect is ascribable to the modification of the scattering background (see Discussion).

Figure 3 reports the DRS spectra of an experiment conceived to verify the stability and the reversibility of Ti-peroxo species. Curves 1 and 2 report the already described spectra collected before and after contact with the H_2O_2/H_2O solution, while spectrum 3 reports the effect of a long elapsed time (15 days in air). A second and a third contact with H_2O_2/H_2O solution drops are reported in curves 4 and 6, respectively, together with the intermediate aging of 1 day after the second contact (curve 5). Curves 2, 4, and 6 are very similar in both LMCT and NIR regions. Curve 3 exhibits an LMCT profile very close to that obtained after activation in vacuo for 0.5 h at 393 K (not reported). Surprisingly a nonnegligible absorption in the 250−485-nm range (40000−20600 cm^{-1}) is still present. Spectra of the aged samples (3 and 5) are considerably different in the region around 385 nm (26 000 cm^{-1}) while they exhibit a similar profile in the 250−300-nm (40000−33300 cm^{-1}) range, which is completely different from that found in spectrum 1. Note that spectrum 3 is obtained on a dried sample, as revealed by the NIR region that is almost the same as that found in spectrum 1. The clear difference observed with respect to spectrum 1 (UV region) is reflecting the presence of new species, only reversible upon calcination at 673 K. Conversely, a similar component observed in the TS-1/H_2O system is distinguishable only at high water content (see arrow in Figure 1) and disappears rapidly with aging. DRS experiments on the stability of the Ti-peroxo complex upon activation in vacuo of the sample at increasing temperatures have also been performed. Corresponding spectra have been omitted for brevity, but qualitative results have been summarized in Table 2 (last rows).

3.2. EXAFS and XANES Spectroscopies. The EXAFS signal of the TS-1/H_2O/H_2O_2 system obtained as described in the Experimental Section is completely different from that obtained in vacuo: see curves 1 and 2 in Figure 4a, where the k^3-weighted, phase-uncorrected FT of TS-1 and TS-1/H_2O/H_2O_2 are reported. While the former exhibits a single, intense, and well-defined first shell peak at 1.43 Å, the latter exhibits two distinct maxima at 1.36 and 1.91 Å which intensity has been strongly dumped by the destructive interference of at least two different signals. Also the second shell has been deeply modified. The same holds for the inset reporting the corresponding curves transformed back into k-space in the range reported in the 7th column of Table 1 ($k\chi(k)$ functions).

The pellet containing the TS-1/H_2O/H_2O_2 system was extracted from the cryostat and left in air for 24 h, turning cream. Inserting the pellet again in the cryostat according to the same procedure and measuring again resulted in the spectrum reported in curve 3 of Figure 4a. The obtained Fourier transformed signal is similar to that measured in vacuo and virtually indistinguishable from that obtained by dosing water on TS-1 (compare dotted (5) and full line (3) spectra in the inset).[29] Once the cryostat again reached room temperature, the pellet was contacted with a drop of water, assuming again its yellow color (as determined from the DRS study). Once cooled again, the sample results in the Fourier transformed signal reported in spectrum 4 of Figure 4a, which, on superficial grounds, is intermediate to spectra 2 and 3.

Part b of Figure 4 reports the XANES region of the X-ray absorption spectra collected in the same experiments. TS-1 in vacuo is characterized by a sharp and intense preedge peak (corresponding to the electronic transition from 1s to hybridized 3p,3d orbitals) at 4967 eV and by a white line at 5004 eV (curve 1). The TS-1/H_2O/H_2O_2 system has a completely different XANES region characterized by a much broader and less intense preedge feature and by a splitting of the white line peak now at 4984 and 4995 eV, which are considerably red shifted and increased in intensity with respect to spectrum 1. These features are lost in spectrum 3 (collected after 24 h) but appear again, although less strong, in spectrum 4 (after contact with water). Table 1 reports a summary of the main XANES features (columns 2−5) as well as the first shell bond distances (R) and coordination numbers (N) and relative Debye−Waller factors (columns 8, 9, and 10) obtained after EXAFS data analysis. It is clear that the here presented EXAFS study has only a preliminary character since it is based on a first shell analysis only. Notwithstanding this fact the phenomenological finger-

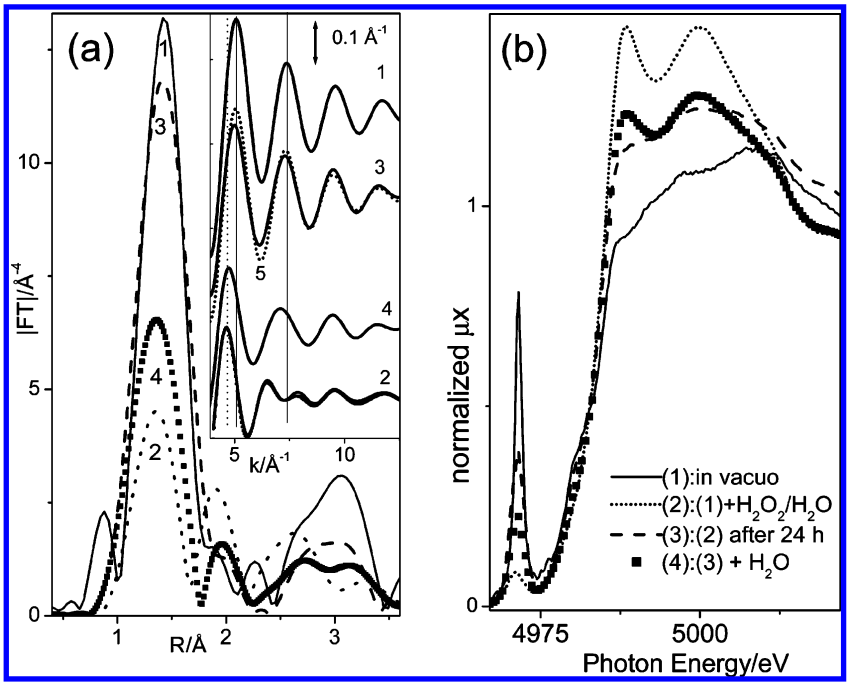

Figure 4. (a) k^3-weighted, phase uncorrected, $\chi(k)$ functions of the TS-1 catalyst during an experiment analogous to that monitored with DRS spectroscopy (Figure 2). Sample as such, curve 1; after contact with H_2O_2/H_2O solution (60%), curve 2. Curve 3 reports the effect of time elapse (24 h). Curve 4 refers to the spectrum collected after spectrum 3 upon contact with H_2O. Spectrum 1 has been collected at room temperature while spectra 2−4 where acquired at liquid nitrogen temperature. The inset reports the back-FT in *k*-space in the interval described in the 7th column of Table 1 of curves 1−4 ($k\chi(k)$ functions). Superimposed to curve 3 is the curve of TS-1 in interaction with H_2O (labeled as curve 5) while superimposed to curve 2 is its best fit. (b): As in part a for the XANES region.

TABLE 1: Summary on the Preedge and White Line Data (XANES) and on the First Shell EXAFS Results of the Data Shown in Figure 5[a]

spectrum: conditions	preedge intensity	preedge fwhm (eV)	white line intensity	white line position (eV)	shell	back-FT range ΔR (Å)	R (Å)	N ±10%	σ (Å) ±15%
(1): in vacuo	0.79	1.4	1.14	5004	framework oxygen	1.01−1.85	1.79 ± 0.01	4	0.05
(2): $+H_2O/H_2O_2$	0.09	3.4	1.46 (1.45)	4984 (4995)	framework oxygen	0.82−2.20	1.83 ± 0.02	2.8	0.07
					peroxo oxygen		2.01 ± 0.02	2	0.05
(3): (2) after 24 h	0.38	2.6	1.25	4996	framework oxygen	1.01−1.85	1.82 ± 0.01	4	0.05
(4): (3) + H_2O	0.23	2.8	1.24 (1.28)	4984 (4994)					

[a] Experimental EXAFS functions have been FT transformed in *R* space in the 3.2−14.3 Å^{-1} range and back-FT into *k*-space, using the ΔR interval listed in the 7th column. Spectra (2) and (4) exhibit a doublet in the edge, so in columns 4 and 5, two values have been reported. For spectrum (2) a two shell fit has been mandatory. The EXAFS data analysis of spectrum (4) has not been performed owing to the heterogeneity of the Ti(IV) species in such conditions. In the EXAFS data analysis shifts of the edge position (up to 1 eV) have also been observed; however, being the instrumental resolution is of the same magnitude, such shifts have not been reported.

prints of the Ti(OO) complex formed in TS-1 in both *R*- and *k*-spaces have been highlighted for the first time.

3.3. Resonant Raman Spectroscopy. The Raman spectra of TS-1 before and after interaction with H_2O_2/H_2O solution have been recently reported and discussed in ref 13. Interaction with H_2O_2 causes (i) the reduction and the blue shift of the Ti-specific 960-cm^{-1} mode, now at 976 cm^{-1}, (ii) the quenching of the 1125-cm^{-1} mode, due to a rupture of the local T_d-like symmetry,[12] (iii) the appearance of the strong and sharp (O−O) stretching mode at 875 cm^{-1}, due to H_2O_2/H_2O solution physisorbed into the zeolite channels, and (iv) the appearance of a strong and complex new feature centered at 618 cm^{-1}. Features i−iii are also observed when the same experiment is performed with a 1064 nm (9400 cm^{-1}) laser source. Conversely, the 618-cm^{-1} band is peculiar of Raman spectra obtained with the 442-nm exciting source, and it is thus ascribed to a Raman-enhanced vibration mode of the side-on Ti-peroxo complex on the basis of a blank experiment performed with $(NH_4^+)_3(TiF_5O_2)^{3-}$ model compound.

3.4. Active Oxygen Content. When the TS-1 is stirred with aqueous solutions of hydrogen peroxide, it retains some active oxygen, i.e. oxygen that can be transferred to suitable reducing agents including iodide ions, thus allowing it to be determined by iodometric titration. In such iodometric titrations of TS-1 samples treated with hydrogen peroxide, however, the problem arises of distinguishing between the active oxygen bound to titanium atoms and physisorbed hydrogen peroxide. To obtain meaningful results, experiments have been run on both Ti-free silicalite-1 (which remains white upon treatment with hydrogen peroxide) and TS-1 samples. It turned out that a gentle washing with water (e.g., 8−10 mL per g of silicalite-1 or TS-1 treated with 1% hydrogen peroxide) on a sintered glass filter easily removes all the titrable oxygen from silicalite-1 (reasonably, physisorbed hydrogen peroxide), whereas TS-1 still retains some active oxygen, which is much more gradually released and which can be assumed to be bound to titanium atoms. The amount of this active oxygen increases with the concentration of the hydrogen peroxide solution but, after the described washing, in no case has it been found higher than one active oxygen atom (corresponding to one peroxo group) per titanium atom. Preliminary stoichiometric experiments indicate that most of this active oxygen can be transferred to suitable organic

TABLE 2: Experimental Values of the DRS Function Measured at 1400 and 385 nm for the Whole Set of Spectra Reported in Figures 2-4: The Notation (*N*/*m*) Means *m*th Spectrum of Figure *n*[a]

figure/ spectrum	sample conditions	$DRS(1400)_{exp}$ (%)	$DRS(385)_{exp}$ (%)	$DRS(385)_{background}$ (%)	$DRS(385)_{Ti\cdots O_2H_2}$ (%)
(2/1)	in air	60	93	94	99
(2/2)	(2/1) +H_2O_2/H_2O	12	10	57	18
(2/3)	(2/2) after 10 h	14	16	59	27
(2/4)	(2/2) after 24 h	22	35	69	51
(2/5)	(2/4) + H_2O	10	24	54	44
(3/1)	in air	60	94	94	100
(3/2)	(3/1) + H_2O_2/H_2O	40	28	86	32
(3/3)	(3/2) after 15 days	65	72	95	76
(3/4)	(3/3) + H_2O_2/H_2O	46	35	90	39
(3/5)	(3/4) after 24 h	56	60	93	64
(3/6)	(3/5) + H_2O_2/H_2O	44	33	89	37
(*x*/1)	in air	61	94	94	100
(*x*/2)	(*x*/1) + H_2O_2/H_2O	40	28	87	32
(*x*/3)	(*x*/2) after 24 h	57	63	93	68
(*x*/4)	(*x*/3) outgassed at 393 K for 30 min	62	72	94	77
(*x*/5)	(*x*/4) calcined at 673 K for 2 h	68	92	95	97

[a] When $n = x$ we refer to an experiment described in the text, the corresponding spectra of which have not been reported for brevity. The measured $DRS(1400)_{exp}$ value allows us to extrapolate, for each spectrum, the value of $DRS(385)_{background}$, representing the loss of reflectivity caused by the presence of water within the crystallites according to the experimental relationship reported in the inset of Figure 1. Finally, the renormalized $DRS(385)_{Ti\cdots O_2H_2}$ value is computed according to eq 2.

TABLE 3: Geometric Features of the $Ti(OSi)_4$ Moieties in the Optimized Bare MFI_T16 and H_2O_2/MFI_T16 Clusters

MFI_T16	Ti−O (Å)	Δ⟨Ti−O⟩ (Å)	α (deg)	β (deg)	Ti−CM (Å)	Ti−O−Si (deg)	Ti−Si (Å)	Ti−L (Å)	BE (kJ mol^{-1})	BE[c] (kJ mol^{-1})
bare	1.797−1.813		110.5−111.3	106.4−109.4	0.559	146.2, 151.3, 168.6, 169.5	3.306−3.426			
+H_2O_2	1.799−1.863	0.019	114.9−116.4	100.8−103.0	0.388	142.7, 152.1, 160.0, 174.0	3.324−3.387	2.44	38.2	21.8

[a] The energetic of the adsorption of H_2O_2 is also listed. Ti−L represents the shortest Ti−O(H_2O_2) distance.

substrates (results not shown). Upon repeated washing, however, even the active oxygen content of the TS-1 samples gradually decreases, until reaching a constant value corresponding to an active oxygen/titanium molar ratio lower than 0.1. The recovered washing water contains hydrogen peroxide in amounts quite comparable to those of the active oxygen lost by the TS-1, thus suggesting that an equilibrium occurs between a titanium-bound oxidizing species and the hydrogen peroxide in the aqueous solutions. After such repeated washings, a distinct yellow color of the TS-1 is no longer appreciated and the powder has, rather, a cream color. The residual active oxygen, although still titrable with iodide ions, appears to be poorly reactive toward organic substrates. Prolonged drying of the TS-1 under reduced pressure also results in the decrease of the active oxygen content, down to this active oxygen/titanium molar ratio lower than 0.1.

Either after repeated washing or prolonged drying, the TS-1 active oxygen is completely lost, and its spectral properties are completely restored, upon calcination at 673 K.

3.5. Ab Initio Study. As described in the Experimental Section, the cluster MFI_T16 (see Figure 5a) has been employed to simulate the Ti(IV) site in TS-1 and to study its interaction with a single H_2O_2 molecule. As far as the TS-1 in a vacuum is concerned, geometrical features of the bare, fully optimized, cluster are listed in Table 3, and are in general good agreement with the experimental data from EXAFS analysis in terms of Ti−O and Ti−Si first and second shell distances and Ti−O−Si angles[14,15,17,20] (see section D of ref 32 for a more detailed comparison).

A single hydrogen peroxide interacts with Ti(IV) center via one of the two O atoms, as shown in Figure 5b, where the optimized H_2O_2/MFI_T16 complex is reported. The insertion of a ligand molecule causes an elongation of the Ti−O bond, averaged over the four framework atoms, of 0.019 Å, see Table 3. A tilted geometry of the adsorbed molecule is reached showing two markedly different Ti···O(H_2O_2) distances of 2.44 and 3.34 Å. The O−O of the H_2O_2 molecule undergoes a shortening, passing from 1.454 to 1.446 Å, while the O−H distance is split from the 0.967 Å equivalent value of the bare molecule to 0.969 and 0.980 Å. Notice that the longer O−H distance refers to the hydrogen atom of the H_2O_2 molecule, which is interacting via H-bond (see also Figure 5b) with one of the three O_{eq} atoms of the [TiO_4] moiety. The distance between the H(H_2O_2) atom and O_{eq} is 1.87 Å. The final ONIOM computed binding energy is low and passes from 38.2 to 21.8 kJ mol^{-1} when BSSE is taken into account. The weak interaction energy and the modest change in the O−O distance induced by the interaction with Ti allows the conclusion that the complex Ti(H_2O_2) is not explaining data deriving from UV−vis, Raman, and EXAFS spectroscopies. In other words, the molecular complex can, at most, be considered only as the precursor of more stable species (as in Scheme 3) formed via a more complex

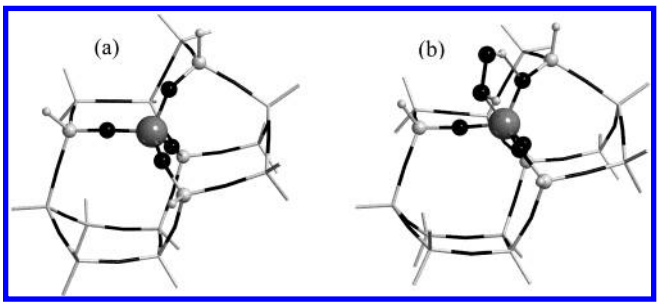

Figure 5. Optimized bare MFI_T16 and MFI_T16/H_2O_2 clusters, parts a and b, respectively. The sticks and balls vs the sticks notation discriminates the model zone (where the link H atoms are omitted for clarity) from the complementary part of the cluster treated at a low level only. Gray, black, and white define Ti, O, and (Si or H) atoms.

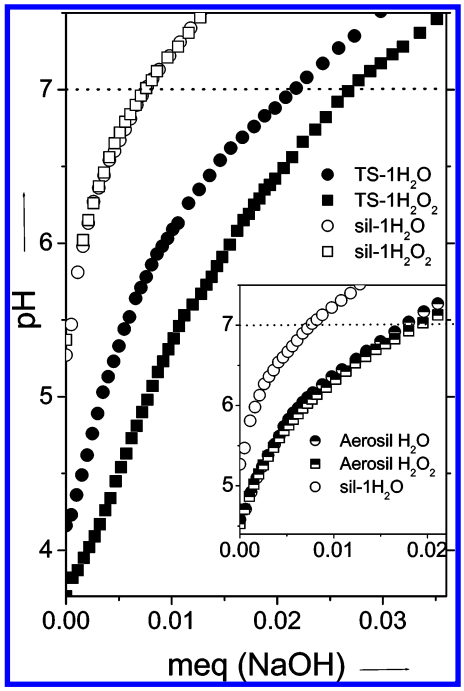

Figure 6. pH values vs added NaOH (mequiv) during the titration experiments performed on TS-1 (full symbols) and on Silicalite-1 (open symbols) in the presence (squares) and in the absence (circles) of H_2O_2. The inset reports the results of the same experiment performed on the Aerosil material (half-open simbol) in the presence (squares) and in the absence (circles) of H_2O_2. For comparison, the data concerning silicalite-1 in the absence (circles) of H_2O_2 have been reported.

mechanism requiring the interaction of other molecules (for instance water).

3.6. The Acidity of the TS-1/H_2O_2/H_2O System. The characterization of the acidity of solid acids by means of titration in aqueous medium has been widely used in the past.[53] To measure H^+ species at the electrode, an ion exchange equilibrium with an additional salt must be present to displace the H^+ species from the internal surface to the solution. The main limitations of the technique are the following: (i) it cannot distinguish Lewis from Brønsted acidity; (ii) it cannot detect acid sites weaker than water itself; and (iii) the actual pH measured depends on the ion exchange equilibrium (nature and concentration of the salt). For these reasons aqueous titrations are inadequate for the characterization of most of the zeolitic acid catalysts working in anhydrous conditions, where spectroscopic methods are preferred.[55] In the case of TS-1, however, which is mainly used in aqueous medium, such titrations are able to yield meaningful, although averaged, information on the acidity of the catalyst in working conditions.

The results of the titration experiments are reported in Figure 6. Two important parameters can be directly extracted from the data reported: (i) the pH value at zero NaOH addition, which is a measure of the relative strength and abundance of the acid sites in the different solids (hereafter pH_0), and (ii) the amount of NaOH needed to reach pH 7.0, which reflects the amount of acidic sites (hereafter B_{pH7}).[53,54] It is apparent that the acidity of silicalite-1 and TS-1 is remarkably different. This difference becomes even greater when the two solids are titrated in the presence of H_2O_2. In pure water TS-1 has two main acidic sites, which are due to water molecules bound to Ti(IV) Lewis sites and to silanols, mainly located in the internal defective nests.[56] Only the latter are present in silicalite-1, which explains both its higher pH_0 5.3 (vs. 4.2) and its lower B_{pH7} values 0.0075 (vs 0.022) mequiv (NaOH).

Addition of H_2O_2 to silicalite-1 does not modify the titration curve (compare open circles with open squares). This means that no additional acidic sites appear in the silicalite-1 system upon adding H_2O_2, i.e., that hydrogen peroxide molecules coordinated to internal silanol do not modify their acidity. This observation is in agreement with the fact that the acidity of H_2O_2 itself is very low. A blank titration experiment (not reported) on a H_2O_2/H_2O solution (0.032 M) resulted in $pH_0 = 5.9$ and $B_{pH7} = 0.0008$ mequiv (NaOH).

Conversely, addition of H_2O_2 to TS-1 moves the whole titration curve toward lower pH values, in particular, pH_0 moves from 4.2 to 3.7 and B_{pH7} moves from 0.022 to 0.027 mequiv (NaOH). This means that the acidity of the TS-1/H_2O_2/H_2O system is remarkably enhanced with respect to the acidity of the two separate systems (H_2O_2/H_2O and TS-1/H_2O). This fact is very important since it reflects the acidity of the catalyst in working conditions. The inflection points observed in the titration curves of both TS-1/H_2O_2/H_2O and TS-1/H_2O, although small, are perfectly reproducible and must thus contain meaningful information. They are due to the presence of acidic sites of different strength, which are saturated at different stages of the titration curve. For the time being we are unable to assign these species.

Summarizing, the increased acidity of the TS-1/H_2O_2/H_2O system must be ascribed to a peculiar interaction between hydrogen peroxide and Ti(IV) centers. To validate this picture two additional blank experiments have been performed an high surface area SiO_2 material (Aerosil 300), containing silanols as unique acidic sites (like silicalite-1), see inset of Figure 6. Due to the higher surface area (300 $m^2\ g^{-1}$), a higher number of acidic sites is present with respect to silicalite-1 (compare empty with half-full circles in the inset). As was the case for silicalite-1, addition of H_2O_2 molecules does not result in an increase of the acidity of the system (compare half-full circles and squares).

4. Discussion

4.1. On the Stability of Ti-Peroxo Species: A DRS, EXAFS/XANES, and I_2 Titration Study. The experiment reporting the DRS spectra of TS-1 as a function of the degree of sample hydration (Figure 1) has been used to obtain a curve reporting the background level at $\lambda = 385$ nm as a function of the DRS component at 1400 nm (2ν(OH)), see inset in Figure 1. This level is only due to the modification of the scattering profile of the sample induced by the presence of liquid water, the TS-1/H_2O system showing no adsorption at $\lambda = 385$ nm. The curve reported in the inset of Figure 1 can be used as an internal calibration of the scattering profile for the TS-1/H_2O_2/H_2O system, where the adsorption from the Ti-peroxo complexes also contributes to the reduction of the measured DRS(385) value. For the TS-1/H_2O_2/H_2O system Table 2 reports the experimental $DRS(1400)_{exp}$ value (3rd column), from which we can estimate the background level of the DRS spectra at $\lambda = 385$ ($DRS(385)_{background}$, 5th column). This value can be used to normalize the experimental DRS(385) value to single out the fraction due to the absorption of the Ti-peroxo complex according to equation

$$DRS(385)_{Ti\cdots O_2H_2} = DRS(385)_{exp}[100/DRS(385)_{background}] \quad (2)$$

The proportionality factor $[100/DRS(385)_{background}]$ therefore takes into account the fraction of photons that does not reach the detector because of scattering (and not absorption) phenomena. The estimated values have been collected in the last

column of Table 2 for all the spectra reported in Figures 2 and 3. For each spectrum, the difference between 100% and DRS-$(385)_{Ti\cdots O_2H_2}$ will give a qualitative estimate of the abundance of the Ti-peroxo species absorbing at 385 nm. In that table, and in the following, the notation (*n*/*m*) means *m*th spectrum of Figure *n* ($n = 2$ and 3).

In the two experiments the spectrum collected before H_2O_2/H_2O dosage, spectra (2/1) and (3/1), yields values between 99% and 100% testifying to the absence of Ti-peroxo species. In the first experiment (Figure 2), the $DRS(385)_{Ti\cdots O_2H_2}$ value increases from 18%, through 27%, to 51% by moving from the as contacted sample (2/2), to that obtained after 10 h (2/3) or 24 h (2/4), reflecting the consumption of the Ti-peroxo complex. Addition of water (2/5) partially restores the original yellow color and the $DRS(385)_{Ti\cdots O_2H_2}$ value decreases again down to 44%, indicating a restoring of the Ti-peroxo complexes.

The same effect is monitored by both EXAFS and XANES spectroscopies (Figure 4a,b). The qualitative view of the k^3-weighted, phase-uncorrected FT of the aged TS1/H_2O_2/H_2O system after addition of water (spectrum 4) partially restores the components at 1.36 and 1.91 Å peculiar to the Ti-peroxo complex, well visible in the as contacted sample (spectrum 2) and disappearing after 24 h (spectrum 3). The same holds for the 4984 and 4995 eV components defining the XANES edge of the sample after contact with the H_2O_2/H_2O solution. This combined DRS and X-ray absorption study can be interpreted in terms of the need of an excess of water to stabilize, inside TS-1, the Ti-peroxo complexes responsible for the 385-nm LMCT. This fact agrees well with the fact that ab initio calculation of the interaction of a single H_2O_2 molecule (i.e., a model where the co-presence of water is not taken into account) with the Ti(IV) site embedded in a zeolitic cluster is not able to explain either the spectroscopic or the structural features of the peroxo complex formed in the TS-1/H_2O_2/H_2O system.

It is remarkable to observe that, despite the lability of most of the Ti-peroxo complexes, a minor fraction of them is still present even after a long contact time (15 days: spectrum (3/3), $DRS(385)_{Ti\cdots O_2H_2} = 76\%$) or after thermal treatment in vacuo for 0.5 h at 393 K (spectrum (*x*/4), $DRS(385)_{Ti\cdots O_2H_2} = 77\%$). These resistant species could correspond to those measured by I_2 titration after several H_2O washes and represent a minority of the whole $Ti\cdots O_2H_2$ complex (less than 10%). This low fraction explains why they did not affect appreciably the X-ray absorption spectra, curves 3 in Figure 4a,b, which are rather close to those measured when only water is dosed on TS-1.[29]

We come back now to the observation that upon H_2O dosage on a sample previously contacted with H_2O_2 and then aged for 24 h, we observe a partial restoration of the peroxo complex absorbing at 385 nm. This suggests that, at least partially, the disappearance of the color is not only related to the fact that H_2O_2 progressively decomposes. Conversely, as a consistent fraction of the peroxo complex absorbing at 385 nm is restored upon H_2O addition, we suggest the existence of equilibria among at least two species, one of them being the η^2 peroxo complex (associated with the yellow color) stabilized by an excess of water. The quite transient character of the Ti-peroxo complex responsible of the 385-nm band is also in agreement with ab initio computations showing that an isolated H_2O_2 molecule forms only a weakly bonded adduct with Ti(IV) species embedded in a zeolitic framework ($BE^c = 21.8$ kJ mol^{-1}). On speculation, it could be tentatively inferred that the cooperative effect of H_2O molecule(s) is important in the stabilization of the peroxo complex as evidenced by UV−vis, EXAFS, and XANES spectroscopies. Unfortunately, the inclusion of one or more H_2O molecules in the cluster is not easily feasible, because they will interact also with the external part of the cluster, treated at a lower computational level in the ONIOM scheme. This means that to avoid any artifacts in the calculation, the whole cluster should be treated at the high level of the theory, implying a dramatic increase of the computational resources required.

4.2. On the Structure of the Yellow Ti-Peroxo Species: An EXAFS and Resonant Raman Study. EXAFS spectroscopy shows us that the local environment of Ti(IV) species is strongly perturbed by the formation of $Ti\cdots O_2H_2$ species, as the signal of the TS-1 and TS-1/H_2O/H_2O_2 systems are completely different (Figure 4). The $k\ \chi(k)$ function of TS-1 in vacuo (curve 1 in the inset of Figure 4a) exhibits a well-defined sinusoidal-like signal typical of a uniform family of scattering atoms in the first coordination sphere around Ti(IV) at 1.79 Å. Conversely, in the case of the TS-1/H_2O/H_2O_2 system, the first shell filtered $k\ \chi(k)$ function is dominated by strong beats caused by the interference between two distinct EXAFS signals, the former being that of the "residual" oxygen framework atoms now located at 1.83 Å (around three). We speak about "residual" because the fit of the experimental data suggests, for framework oxygen, a coordination number close to three. The O−O moiety is strongly adsorbed (low Debye−Waller factor) in a side-on geometry where both O atoms are located at a Ti−O distance of 2.01 Å (see Table 1). In conclusion, EXAFS data are more compatible with the formation of a side-on peroxo complex starting from a defect site (Scheme 3 b) or from a site created via hydrolysis of a Ti−O−Si bridge (Scheme 3a). Following Schemes 3 and 4, the hypothesis of a deprotonated Ti−OO complex is supported, although indirectly, by the remarkable increase of the acidity of the TS-1/H_2O/H_2O_2 system (see Figure 6).

The EXAFS model is in agreement with the results of the resonant Raman study where the nature of the peroxo species responsible for the 385-nm component has been recently highlighted.[13] With use of a 442 nm (22 625 cm^{-1}) laser source, which is on the low energy tail of the LMCT band around 385 nm (26 000 cm^{-1}) of the TS-1/H_2O_2/H_2O system, the resonant enhanced response from vibrational modes of the peroxo complex has been observed. Under such conditions, a new band (scarcely visible when a near-IR laser is used) at 618 cm^{-1} has been observed. A similar enhancement has been observed on the $(NH_4^+)_3(TiF_5O_2)^{3-}$ model compound formed by the packing of TiF_5O_2 units intercalated by the NH_4^+ counterions (absorption centered at 595 cm^{-1}). The similarity between the spectroscopic features, both UV−vis of $(NH_4^+)_3(TiF_5O_2)^{3-}$ and TS-1/H_2O_2/H_2O systems, allowed us to conclude that the species responsible for the band at 26 000 cm^{-1} (385 nm) of the TS-1/H_2O_2/H_2O system is a "side-on" Ti-peroxo species characterized by a Raman mode at 618 cm$^{-1,}$ which is resonance enhanced by an exciting laser line falling in the LMCT transition.[13]

The geometry optimized by ab initio simulation is far from being side-on, showing two markedly different $Ti\cdots O(H_2O_2)$ distances at 2.44 and 3.44 Å. These distances reflect a weak interaction between the Ti center and neutral H_2O_2. This cannot explain the UV−vis, Raman, and EXAFS data. We think that the discrepancy between experiment and computation reflects the inadequacy of the adopted model. More complex situations are now being investigated, either by considering the role of water molecules in the stabilization of the peroxo complex or by considering adducts with a partially or totally deprotonated molecule or both.

4.3. On the Role Played by the Acidity in the TS-1/H_2O_2/H_2O System. The experiments illustrated in Figure 6 show

SCHEME 5

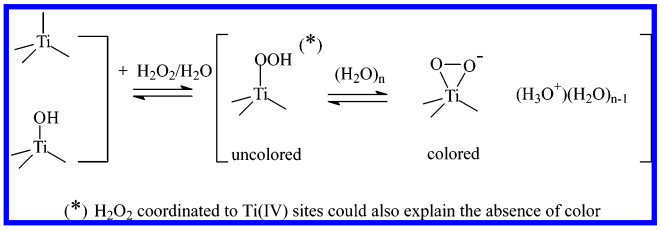

definitely that TS-1/H_2O is slightly more acidic than the Silicalite-1/H_2O counterpart and that TS-1/H_2O/H_2O_2 shows strongly enhanced acidity with respect to the Silicalite-1/H_2O/H_2O_2 reference counterpart. The slight enhancement of the acidity of the TS-1/H_2O system is likely related to the coordination of water to Ti centers, which is accompanied by a modest polarization of the OH bond. The strong enhancement of the acidity of the TS-1/H_2O_2/H_2O system with respect to the TS-1/H_2O one is remarkable. Addition of hydrogen peroxide causes a decrease of pH_0 from 4.2 to. 3.7 and an increase of the B_{pH7} value from 0.022 to 0.027 mequiv (NaOH). As the addition of H_2O_2 in the parent Ti-free silicalite-1/H_2O system does not affect the two abovementioned parameters, a synergic role between Ti(IV) centers and hydrogen peroxide must be invoked. These data find a simple explanation by assuming that TiOOH species formed following either Schemes 2a,b or 3a,b are the acidic species detected during the titration experiments.

5. Conclusions and Open Questions

The stability of the peroxo complex, well characterized by Resonant Raman spectroscopy, has been followed by UV−vis and XAFS measurements in relation to aging time and H_2O_2 content. The yellow species (385-nm band) with η^2 structure is stable only in the presence of an excess of water. Water removal causes the transformation of colored peroxo groups into uncolored ones. This process is reversible indicating that water molecules play a key role in determining the ratio between hydroperoxo and peroxo species. This suggests that the affinity of the H_2O_2 molecule to form a complex with Ti(IV) in TS-1 is very low in the absence of the cooperative effect of H_2O molecules. In Scheme 5 a sketch of previously described species involving a Ti site previously generated by hydrolysis is illustrated.

The observation that this peroxo species can be restored upon further addition of H_2O_2 indicates that the interaction with H_2O_2 does not cause any evident extensive damage to the Ti(IV) structure. Only a small fraction (about 10%) of Ti(IV) is involved in the formation of different, very stable species (cream colored) which are eliminated only upon activation at 673 K. A similar percentage of them have been found also by iodometric titration. As briefly discussed in section 3.4, these residual stable species are poorly reactive toward organic substrates.

It has been shown that the acidity of the TS-1/H_2O solid is strongly enhanced by addition of H_2O_2. This fact has to be taken into account in the reactivity of the catalyst. An increased acidic character of TS-1 with respect to pure Silicalite-1 has been stated together with the observation of an enhanced acidic character upon H_2O_2 addition.

Acknowledgment. The present work is a part of a project coordinated by A. Zecchina and co-financed by the Italian MURST (Cofin 2000, Area 03). We are indebted to F. X. Llabrés i Xamena for fruitful discussion. We thank the team of the EXAFS 13 beamline at LURE DCI synchrotron (in particular F. Villain) for important and friendly support during XANES and EXAFS measurements.

References and Notes

(1) Taramasso, M.; Perego, G.; Notari, B. U.S. Patent No. 4410501, 1983. TS-1 is a microporous titanosilicate showing a three-dimensional pore system consisting of two intersecting sets of tubular channels (ca. 5.5 Å in diameter) defined by 10-member rings of TO_4 tetrahedra (T = Si or Ti). TS-1 is the Ti-analog of ZSM-5 aluminosilicate (zeolite), exhibiting the MFI structure (IUPAC nomenclature).

(2) (a) Meier, W. M.; Olson, D. H.; Baerlocher, C. *Atlas of Zeolite Structure Types*; Elsevier: London, UK, 1996. (b) Thomas, J. M.; Bell, R. G.; Catlow, C. R. A. In *Handbook of Heterogeneous Catalysis*; Ertl, G., Knözinger, H., Weitkamp, J., Eds.; VCH: Weinheim, Germany, 1997; pp 286−310.

(3) (a) Clerici, G. M. *Appl. Catal.* **1991**, *68*, 249−261. (b) Clerici, G. M.; Bellussi, G.; Romano, U. *J. Catal.* **1991**, *129*, 159−167. (c) Bellussi, G.; Carati, A.; Clerici, G. M.; Maddinelli, G.; Millini, R. *J. Catal.* **1992**, *133*, 220−230. (d) Mantegazza, M. A.; Leofanti, G.; Petrini, G.; Padovan, M.; Zecchina, A.; Bordiga, S. *Stud. Surf. Sci. Catal.* **1994**, *82*, 541−550. (e) Mantegazza, M. A.; Petrini, G.; Spanò, G.; Bagatin, R.; Rivetti, F. *J. Mol. Catal. A* **1999**, *146*, 223−228. (f) Clerici, G. M. *Top. Catal.* **1991**, *15*, 257−263.

(4) Notari, B. *Adv. Catal.* **1996**, *41*, 253−334 and references therein.

(5) (a) Millini, R.; Previdi Massara, E.; Perego, G.; Bellussi, G. *J. Catal.* **1992**, *137*, 497−503. (b) Lamberti, C.; Bordiga, S.; Zecchina, A.; Carati, A.; Fitch, A. N.; Artioli, G.; Petrini, G.; Salvalaggio, M.; Marra, G. L. *J. Catal.* **1999**, *183*, 222−231. (c) Marra, G. L.; Artioli, G.; Fitch, A. N.; Milanesio, M.; Lamberti, C. *Microporous Mesoporous Mater.* **2000**, *40*, 85−94. (d) Lamberti, C.; Bordiga, S.; Zecchina, A.; Artioli, G.; Marra, G. L.; Spanò, G. *J. Am. Chem. Soc.* **2001**, *123*, 2204−2212. (e) Milanesio, M.; Artioli, G.; Palin, L.; Gualtieri, A. F.; Lamberti, C. *J. Am. Chem. Soc.* **2003**, *125*, 14549−14558.

(6) Tozzola, G.; Mantegazza, M. A.; Ranghino, G.; Petrini, G.; Bordiga, S.; Ricchiardi, G.; Lamberti, C.; Zulian, R.; Zecchina, A. *J. Catal.* **1998**, *179*, 64−71.

(7) Boccuti, M. R.; Rao, K. M.; Zecchina, A.; Leofanti, G.; Petrini, G. *Stud. Surf. Sci. Catal.* **1989**, *48*, 133−144.

(8) Lin, W.; Frei, H. *J. Am. Chem. Soc.* **2002**, *124*, 9292−9298.

(9) Scarano, D.; Zecchina, A.; Bordiga, S.; Geobaldo, F.; Spoto, G.; Petrini, G.; Leofanti, G.; Padovan, M.; Tozzola, G. *J. Chem. Soc., Faraday Trans.* **1993**, *89*, 4123−4130.

(10) Huybrechts, D. R.; Buskens, P. L.; Jacobs, P. A. *J. Mol. Catal.* **1992**, *71*, 129−147.

(11) Li, C.; Xiong, G.; Xin, Q.; Liu, J.; Ying, P.; Feng, Z.; Li, J.; Yang, W.; Wang, Y.; Wang, G.; Liu, X.; Lin, M.; Wang, X.; Min, E. *Angew. Chem., Int. Ed.* **1999**, *38*, 2220−2222.

(12) Ricchiardi, G.; Damin., A.; Bordiga, S.; Lamberti, C.; Spanò, G.; Rivetti, F.; Zecchina, A. *J. Am. Chem. Soc.* **2001**, *123*, 11409−11419.

(13) (a) Bordiga, S.; Damin, A.; Bonino, F.; Ricchiardi, G.; Lamberti, C.; Zecchina, A. *Angew. Chem., Int. Ed.* **2002**, *41*, 4734−4737. (b) Bordiga, S.; Damin, A.; Bonino, F.; Ricchiardi, G.; Zecchina, A.; Tagliapietra, R.; Lamberti, C. *Phys. Chem. Chem. Phys.* **2003**, *5*, 4390−4393.

(14) (a) Bordiga, S.; Coluccia, S.; Lamberti, C.; Marchese, L.; Zecchina, A.; Boscherini, F.; Buffa, F.; Genoni, F.; Leofanti, G.; Petrini, G.; Vlaic, G. *J. Phys. Chem.* **1994**, *98*, 4125−4132. (b) Bordiga, S.; Boscherini, F.; Coluccia, S.; Genoni, F.; Lamberti, C.; Leofanti, G.; Marchese, L.; Petrini, G.; Vlaic, G.; Zecchina, A. *Catal. Lett.* **1994**, *26*, 195−208.

(15) Le Noc, L.; Trong On, D.; Solomykina, S.; Echchahed, B.; Bél, F.; Cartier dit Moulin C.; Bonneviot, L. *Stud. Surf. Sci. Catal.* **1996**, *101*, 611−620.

(16) Zecchina, A.; Bordiga, S.; Lamberti, C.; Ricchiardi, G.; Scarano, D.; Petrini, G.; Leofanti, G.; Mantegazza, M. *Catal. Today* **1996**, *32*, 97−106.

(17) Lamberti, C.; Bordiga, S.; Arduino, D.; Zecchina, A.; Geobaldo, F.; Spanò, G.; Genoni, F.; Petrini, G.; Carati, A.; Villain, F.; Vlaic, G. *J. Phys. Chem. B* **1998**, *102*, 6382−6390.

(18) Trong On, D.; Le Noc, L.; Bonneviot, L. *Chem. Commun.* **1996**, 299−300.

(19) Lamberti, C.; Turnes Palomino, G.; Bordiga, S.; Arduino, D.; Zecchina, A.; Vlaic, G. *Jpn. J. Appl. Phys.* **1999**, *38−1*, 55−58.

(20) Gleeson, D.; Sankar, G.; Catlow, C. R. A.; Thomas, J. M.; Spanó, G.; Bordiga, S.; Zecchina, A.; Lamberti, C. *Phys. Chem. Chem. Phys.* **2000**, *2*, 4812−4817.

(21) Clerici, M. G.; Ingallina, P.; Millini, R. In *Proceedings of the 9th International Zeolite Conference, Montreal, 1992*; von Ballmoos, R., Higgins, J. B., Treacy, M. M. J., Eds.; Butterworth-Heinemann: Boston, MA, 1993; Vol. 1, pp 445−452.

(22) Zecchina, A.; Bordiga, S.; Spoto, G.; Damin, A.; Berlier, G.; Bonino, F.; Prestipino, C.; Lamberti, C. *Topics Catal.* **2002**, *21*, 67−78.

(23) (a) Bolis, V.; Bordiga, S.; Lamberti, C.; Zecchina, A.; Carati, A.; Rivetti, F.; Spanò, G.; Petrini, G. *Langmuir* **1999**, *15*, 5753−5764. (b) Bolis,

V.; Bordiga, S.; Lamberti, C.; Zecchina, A.; Carati, A.; Petrini, G.; Rivetti, F.; Spanò G. *Microporous Mesoporous Mater.* **1999**, *30*, 67−76.

(24) Millini, R.; Perego, G. *Gazz. Chim. Ital.* **1996**, *126*, 133−140.

(25) Vayssilov, G. N.; *Catal. Rev. Sci. Engl.* **1997**, *39*, 209−251.

(26) (a) Geobaldo, F.; Bordiga, S.; Zecchina, A.; Giamello, E.; Leofanti, G.; Petrini, G. *Catal. Lett.* **1992**, *16*, 109−115. (b) Bonoldi, L.; Busetto, C.; Congiu, A.; Marra, G.; Ranghino, G.; Salvalaggio, M.; Spanò, G.; Giamello, E. *Spectrochim. Acta A* **2002**, *58*, 1143−1154.

(27) (a) Chaudari, K.; Srinivas, D.; Ratnasamy, P. *J. Catal.* **2001**, *203*, 25−32. (b) Chaudari, K.; Srinivas, D.; Sivasanker, S.; Ratnasamy, P. *J. Mol. Catal. A: Chem.* **2000**, *162*, 199−207. (c) Srinivas, D.; Manikandan, P.; Laha, S. C.; Kumar, R.; Ratnasamy, P. *J. Catal.* **2003**, *217*, 160−171.

(28) Bonino, F.; Damin, A.; Bordiga, S.; Lamberti, C.; Zecchina, A. *Langmuir* **2003**, *19*, 2155−2161.

(29) Bordiga, S.; Damin, A.; Bonino, F.; Zecchina, A.; Spanò, G.; Rivetti, F.; Bolis, V.; Lamberti C. *J. Phys. Chem. B* **2002**, *106*, 9892−9905.

(30) Damin, A.; Bonino, F.; Ricchiardi, G.; Bordiga, S.; Zecchina, A.; Lamberti, C. *J. Phys. Chem. B* **2002**, *106*, 7524−7526.

(31) Barker, C. M.; Gleeson, D.; Katsoyannis, N.; Catlow, C. R. A.; Sankar, G.; Thomas, J. M. *Phys. Chem. Chem. Phys.* **2002**, *4*, 1128−1240.

(32) Damin, A.; Bordiga, S.; Zecchina, A.; Lamberti, C. *J. Chem. Phys.* **2002**, *117*, 226−237.

(33) Damin, A.; Bordiga, S.; Zecchina, A.; Doll, K.; Lamberti, C. *J. Chem. Phys.* **2003**, *118*, 10183−10194.

(34) (a) Jentys, A.; Catlow, C. R. A. *Catal. Lett.* **1993**, *22*, 251−257. (b) de Man, A. J. M.; Sauer, J. *J. Phys. Chem.* **1996**, *100*, 5025−5034.

(35) (a) Sinclair, P. E.; Sankar, G.; Catlow, C. R. A.; Thomas, J. M.; Maschmeyer, T. *J. Phys. Chem. B* **1997**, *101*, 4232−4237. (b) Sinclair, P. E.; Sankar, G.; Catlow, C. R. A.; Thomas, J. M.; Maschmeyer, T. *J. Phys. Chem. B* **1997**, *101*, 4232−4237.

(36) (a) Zicovich-Wilson, C. M.; Dovesi, R.; Corma, A. *J. Phys. Chem. B* **1999**, *103*, 988−994. (b) Ricchiardi, G.; de Man, A.; Sauer, J. *Phys. Chem. Chem. Phys.* **2000**, *2*, 2195−2204.

(37) Sinclair, P. E.; Catlow, C. R. A. *J. Phys. Chem. B* **1999**, *103*, 1084−1095.

(38) Munakata, H.; Oumi, Y.; Miyamoto, A. *J. Phys. Chem. B* **2001**, *105*, 3493−3501.

(39) Vayssilov, G. N.; van Santen, R. A. *J. Catal.* **1998**, *175*, 170−174.

(40) Karlsen, E.; Schöffel, K. *Catal. Today* **1996**, ***32***, 107−114.

(41) (a) Server, R. R.; Root, T. W. *J. Phys. Chem. B* **2003**, *107*, 4080−4089. (b) Server, R. R.; Root, T. W. *J. Phys. Chem. B* **2003**, *107*, 4090−4099.

(42) (a) Ruzic-Toros, Z.; Kojic-Prodic, B.; Sljukic, M. *Inorg. Chim. Acta* **1984**, *86*, 205−208. (b) Jeske, P.; Haselhorst, G.; Weyhermuller, T.; Wieghardt, K.; Nuber, B. *Inorg. Chem.* **1994**, *33*, 2462−2471. (c) Hagadorn, J. R.; Arnold, J. *Inorg. Chem.* **1997**, *36*, 2928−2929. (d) Hagadorn, J. R.; Arnold, J. *Organometallics* **1998**, *17*, 1355−1368.

(43) (a) Mimmoun, H.; Postel, M.; Casabianca, F.; Fisher, J.; Mitschler, A. *Inorg. Chem.* **1982**, *21*, 1303−1306. (b) Yamase, T.; Ishikawa, E.; Asai, Y.; Kani, S. *J. Mol. Catal. A: Chem.* **1996**, *114*, 237−245.

(44) Gao, F.; Yamase T.; Suzuki, H. *J. Mol. Catal.* **2002**, *180*, 97−108.

(45) Lamberti, C.; Bordiga, S.; Salvalaggio, M.; Spoto, G.; Zecchina, A.; Geobaldo, F.; Vlaic, G.; Bellatreccia, M. *J. Phys. Chem. B* **1997**, *101*, 344−360.

(46) Michalowicz, A. *J. Phys. IV Fr.* **1997**, *7*, C2-235−236.

(47) Lytle, F. W.; Sayers, D. E.; Stern, E. A. *Physica B* **1989**, *158*, 701−722.

(48) (a) Maseras, F.; Morokuma, K. *J. Comput. Chem.* **1995**, *16*, 1170−1179. (b) Humbel, S.; Sieber, S.; Morokuma, K. *J. Chem. Phys.* **1996**, *105*, 1959−1967. (c) Dapprich, S.; Komaromi, I.; Byun, K. S.; Morokuma, K.; Frisch, M. J. *J. Mol. Struct. THEOCHEM* **1999**, *461*, 1−21.

(49) Hay, P. J.; Wadt, W. R. *J. Chem. Phys.* **1985**, *82*, 299−310.

(50) Schaefer, A.; Huber, C.; Ahlrichs, R. *J. Chem. Phys.* **1994**, *100*, 5829−5835.

(51) The Ti−CM distance moves from 0.334 × Ti−O in T_d symmetry (where 0.334 = cos(180−109.5°)) to zero in a perfect bipyramidal symmetry (where the Ti atom lies in the plane defined by the three O_{eq} atoms). As a consequence, the Ti−CM distance gives a direct measure of the symmetry distortion undergone by the TiO_4 moiety upon insertion in a portion of the zeolite framework (model MFI_T16) and upon adsorption of a ligand molecule. For more details see refs 30 and 32.

(52) Lendvay, G.; Mayer, I. *Chem. Phys. Lett.* **1998**, *297*, 365−373.

(53) (a) Tanabe, K. *Solid acid and Bases*; Academic Press: New York, 1970; pp 38−41. (b) Forni L. *Catal. Rev. Sci. Eng.* **1974**, *8*, 65−115. (c) Benesi, H. A.; Winquist, B. H. C. *Adv. Catal.* **1978**, *27*, 97−182.

(54) Strictly speaking, the amount of acidic sites is quantified by the amount of NaOH needed to reach the equivalence point. Due to the heterogeneity of acidic sites and due to the limited pH range that is possible to investigated before hydrolysis reactions take place, the equivalence point cannot be easily singled out. As a consequence we arbitrarily used pH 7.0 as the final point of our titration. The validity of the B_{pH7} value to quantify the amount of acidic sites has been demonstrated by a parallel set of experiments performed with different amounts of sample. In all cases the obtained B_{pH7} value scales with the sample mass within 10%.

(55) Pazé, C.; Bordiga, S.; Lamberti, C.; Salvalaggio, M.; Zecchina, A.; Bellussi, G. *J. Phys. Chem. B* **1997**, *101*, 4740−4751.

(56) (a) Zecchina, A.; Bordiga, S.; Spoto, G.; Marchese, L.; Petrini, G.; Leofanti, G.; Padovan, M. *J. Phys. Chem.* **1992**, *96*, 4985−4990. (b) Zecchina, A.; Bordiga, S.; Spoto, G.; Marchese, L.; Petrini, G.; Leofanti, G.; Padovan, M. *J. Phys. Chem.* **1992**, *96*, 4991−4997. (c) Zecchina, A.; Bordiga, S.; Spoto, G.; Marchese, L.; Petrini, G.; Leofanti, G.; Padovan, M.; Otero Areàn, C. *J. Chem. Soc., Faraday Trans.* **1992**, *88*, 2959−2969. (d) Artioli, G.; Lamberti, C.; Marra, G. L. *Acta Crystallogr. B* **2000**, *56*, 2−10. (e) Bordiga, S.; Ugliengo, P.; Damin, A.; Lamberti, C.; Spoto, G.; Zecchina, A.; Spanò, G.; Buzzoni, R.; Dalloro, L.; Rivetti, F. *Top. Catal.* **2001**, *15*, 43−52. (f) Bordiga, S.; Roggero, I.; Ugliengo, P.; Zecchina, A.; Bolis, V.; Artioli, G.; Buzzoni, R.; Marra, G. L.; Rivetti, F.; Spanò, G.; Lamberti, C. *J. Chem. Soc., Dalton Trans.* **2000**, 3921−3929.